Chemical and Process Engineering Research
ISSN 2224-7467 (Paper) ISSN 2225-0913 (Online)
Vol.28, 2014

Numerical Investigation of the Effects of Reactor Pressure on Biomass Devolatilization in Thermally Thick Regime

Pious O. Okekunle[1*], Daniel I. Adeniranye[1], Emmanuel A. Osowade[2]

1. Department of Mechanical Engineering, Faculty of Engineering and Technology, Ladoke Akintola University of Technology, P.M.B. 4000, Ogbomoso, Oyo state, Nigeria.

2. Department of Mechanical Engineering, Faculty of Technology, Obafemi Awolowo University(O.A.U.), Ile-Ife, Osun state, Nigeria.
*Email of the corresponding author: pookekunle@lautech.edu.ng

Abstract

Effects of reactor pressure on biomass devolatilization in thermally thick regime were numerically investigated in this study. Wood pellet ($\rho = 400\ kg/m^3$, $\emptyset\ 10\ mm$ and length $20\ mm$) was modeled as a two-dimensional porous solid and pyrolysis was simulated at a heating rate of 30 K/s and final reactor temperature of 973 K for five different reactor pressures [vacuum; 0.0001 and 0.01 atm, atmospheric;1 atm and pressurized; 10 and 100 atm, regions]. Transport equations, kinetic models, intra-particle pressure generation equation and energy conservation equation were coupled and simultaneously solved to simulate the pyrolysis process. Solid mass conservation equations were solved by first order Euler Implicit Method. Darcy's law was used to estimate intra-particle flow velocity. Finite Volume Method was used to discretize the transport, energy conservation and pressure generation equations. Results showed that even in thermally thick regime, increase in reactor pressure does not affect the rate of primary tar generation. Findings also revealed that the rates of generation of secondary products at atmospheric and pressurized regions are not significantly different. Further increase in reactor pressure in the pressurized region resulted in a slight reduction in the peak of secondary products generation rate. Results further showed that increase in reactor pressure reduced intra-particle temperature gradient especially in the pressurized region, thereby causing process time elongation. As would be expected, tar release rate decreased with increase in reactor pressure while gas release rate increased in both atmospheric and pressurized regions.

Keywords: Biomass, pyrolysis, pressure effects, thermally thick regime, intra-particle secondary reactions

1. Introduction

The need for alternative sources of energy, which are environmentally friendly, has been realized the world over. Aside from the fact that fossil fuels threaten the environment by emitting greenhouse gases, their reserves are getting depleted. This has made energy analysts uncertain about the possibility of fossils meeting future energy demand. Subsequently, biomass energy has been receiving attention and many research works are still ongoing to explore its potentials. Pyrolysis and gasification are thermochemical routes to recover energy locked up in biomass and agricultural residues. Many research works have been carried out for better understanding of the effects of various process parameters, physical phenomena and sample nomenclature on these processes [1-13]. Of recent, we have investigated the effects of reactor pressure on pyrolysis in thermally thin regime [14]. It was found out that pressure increase within vacuum region (0.0001 - 0.01 atm) and within pressurized region (10 – 100 atm) has no significant effect on the rate of primary tar production, primary tar intra-particle secondary reactions rates, and gas and tar release rates. However, increase in pressure from vacuum to atmospheric, and from atmospheric to pressurized region increased primary tar residence time within the pyrolyzing solid, thereby enhancing intra-particle secondary reactions. In most commercial boilers and gasifiers, biomass samples used are usually within the thermally thick regime [15]. In this regime, there exists a significant intra-particle temperature gradient which will affect various physical phenomena and the kinetics of chemical reactions taking place during pyrolysis. Therefore, this study invesigates the effects of reactor pressure on pyrolysis in thermally thick regime.

2. Pyrolysis Mechanism

Several mechanisms have been developed by researchers to explain various phenomena taking place during biomass pyrolysis [16]. Figure 1 shows the structure of the mechanism adopted in this study. Detailed explanation on the development of this model has been reported in our earlier research works [17,18]. As shown in the figure, wood first decomposes by three endothermic competing primary reactions to form gas, primary tar and intermediate solid. The primary tar undergoes secondary reactions to yield more gas and char. The intermediate solid is further transformed into char by a strong exothermic reaction as shown in the figure. Reaction rates were assumed to follow Arrhenius expression of the form; $k_i = A_i \exp\left({}^{-E_i}/_{RT}\right)$. The chemical kinetic (*A* and *E*) and thermodynamic (*a* and *b*) parameters are as given in one of our previous works [18].

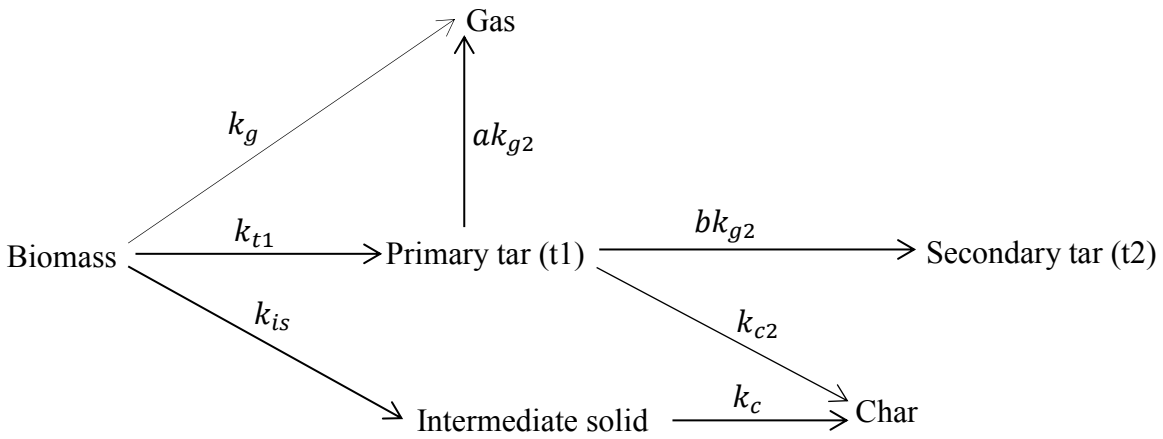

Figure 1: Schematic illustration of the pyrolysis mechanism

3. Numerical Simulation

The governing equations, model assumptions and numerical procedures in this study are already given in our previous studies [17, 18, 19], therefore, fundamental governing equations are only given here.

3.1 Solid mass conservation equation

The instantaneous mass balance of the pyrolyzing solid comprises three endothermic consumption terms yielding gas, tar and intermediate solid:

$$\frac{\partial \rho_s}{\partial t} = -(k_g + k_t + k_{is})\rho_s \quad (1)$$

The intermediate solid instantaneous mass balance equation (equation (2)) contains two terms, one for the conversion of the virgin solid to intermediate solid and the other from exothermic decomposition of intermediate solid to yield char, given as

$$\frac{\partial \rho_{is}}{\partial t} = k_{is}\rho_s - k_c\rho_{is} \quad (2)$$

In the same vein, the char instantaneous mass balance equation (equation(3)) contains two terms, one from the exothermic decomposition of intermediate solid and the other from primary tar secondary reaction to yield char, given as

$$\frac{\partial \rho_c}{\partial t} = k_c\rho_{is} + k_{c2}\rho_t \quad (3)$$

3.2 Mass conservation equations of gas phase components

Mass conservation equations for all gas phase components are expressed by two-dimensional cylindrical coordinate system consisting of both temporal and spatial gradients and source terms

$$\text{Ar: } \frac{\partial(\varepsilon\rho_{Ar})}{\partial t} + \frac{\partial(\rho_{Ar}U)}{\partial z} + \frac{1}{r}\frac{\partial(r\rho_{Ar}V)}{\partial r} = S_{Ar}, \quad (4)$$

$$\text{Gas: } \frac{\partial(\varepsilon\rho_g)}{\partial t} + \frac{\partial(\rho_g U)}{\partial z} + \frac{1}{r}\frac{\partial(r\rho_g V)}{\partial r} = S_g, \quad (5)$$

$$\text{Primary tar : } \frac{\partial(\varepsilon\rho_{t1})}{\partial t} + \frac{\partial(\rho_{t1}U)}{\partial z} + \frac{1}{r}\frac{\partial(r\rho_{t1}V)}{\partial r} = S_{t1}, \quad (6)$$

$$\text{Secondary tar: } \frac{\partial(\varepsilon\rho_{t2})}{\partial t} + \frac{\partial(\rho_{t2}U)}{\partial z} + \frac{1}{r}\frac{\partial(r\rho_{t2}V)}{\partial r} = S_{t2} \quad (7)$$

S_{Ar} , S_g, S_{t1} and S_{t2} are the source terms for the carrier gas, argon, gas, primary tar and secondary tar respectively, and are given by

$$S_{Ar} = 0 \quad (8)$$

$$S_g = k_g\rho_s + \varepsilon k_{g2}\rho_{t1} \quad (9)$$

$$S_{t1} = k_t\rho_s - \varepsilon[k_{c2} + (a+b)k_{g2}]\rho_{t1} \quad (10)$$

$$S_{t2} = \varepsilon b k_{g2}\rho_{t1} \quad (11)$$

Intra-particle tar and gas transport velocity was estimated by Darcy's law,

$$U = -\frac{B}{\mu}\left(\frac{\partial P}{\partial z}\right) \quad (12)$$

$$V = -\frac{B}{\mu}\left(\frac{\partial P}{\partial r}\right) \quad (13)$$

where B and μ are respectively the charring biomass solid permeability and kinematic viscosity. Porosity, ε, is expressed as

$$\varepsilon = 1 - \frac{\rho_{s,sum}}{\rho_{w,0}}(1 - \varepsilon_{w,0}) \quad (14)$$

where $\varepsilon_{w,0}$, $\rho_{s,sum}$ and $\rho_{w,0}$ are the initial porosity of wood, the sum of solid mass density and initial wood density, respectively. The permeability, B, of the charring biomass is expressed as a linear interpolation between the solid phase components, given as

$$B = (1 - \eta)B_w + \eta B_c \quad (15)$$

where η is the degree of pyrolysis and is defined as

$$\eta = 1 - \frac{\rho_s + \rho_{is}}{\rho_{w,0}} \quad (16)$$

3.3 Energy conservation equation

The energy conservation equation is given as

$$\left(C_{p,w}\rho_s + C_{p,w}\rho_{is} + C_{p,c}\rho_c + \varepsilon C_{p,t}\rho_{t1} + \varepsilon C_{p,t}\rho_{t2} + \varepsilon C_{p,g}\rho_g\right)\frac{\partial T}{\partial t} = \frac{\partial}{\partial z}\left(k_{eff(z)}\frac{\partial T}{\partial z}\right) + \frac{1}{r}\frac{\partial}{\partial r}\left(rk_{eff(r)}\frac{\partial T}{\partial r}\right) - l_c\Delta h_c - \sum_{i=g,t1,is} m_i\Delta h_i - \varepsilon\sum_{i=g2,t2,c2} n_i\Delta h_i \quad (17)$$

where

$$l_c = A_c \exp(-E_c/RT)\,\rho_{is} \quad (18)$$

$$m_i = A_i \exp(-E_i/RT)\,\rho_s \quad i = g, t1, is \tag{19}$$

$$n_i = A_i \exp(-E_i/RT)\,\rho_{t1} \quad i = g2, t2, c2 \tag{20}$$

The thermo-physical properties of the wood sample are as given in our recent study [14].

3.4 Pressure evolution

The total pressure is the sum of the partial pressures of the inert gas (argon), gas and secondary tar from the pyrolysis process. It is given as

$$P = P_{Ar} + P_{t2} + P_g;\;\; P_i = \frac{\rho_i RT}{M_i} \qquad (i = Ar, t2, g) \tag{21}$$

where M_i and R are the molecular weight of each gaseous species and universal gas constant, respectively. Combining equations (4), (5), (7), (12), (13) and (24), intra-particle pressure equation was obtained as

$$\frac{\partial}{\partial t}\left(\varepsilon \frac{P}{T}\right) - \frac{\partial}{\partial r}\left[\frac{BP}{\mu T}\left(\frac{\partial P}{\partial z}\right)\right] - \frac{1}{r}\frac{\partial}{\partial r}\left[r\frac{BP}{\mu T}\left(\frac{\partial P}{\partial r}\right)\right] = \frac{R}{M_{t2}}S_{t2} + \frac{R}{M_g}S_g \tag{22}$$

3.5 Numerical Procedure

Wood cylinder was modeled as a two-dimensional isotropic porous solid. Wood pores were assumed to be initially filled with argon. As the solid was pyrolyzed, tar and gas were formed while argon was displaced to the outer region without participating in the pyrolysis reaction. The solid mass conservation equations (eqs (1) – (3)) were solved by first-order Euler Implicit Method. The mass conservation equations for argon, primary tar, gas and secondary tar (eqs (4) – (7)), energy conservation equation (eq. (17)) and the pressure equation (eq. (22)) were discretized using finite volume method. Hybrid differencing scheme was adopted for the convective terms. First-order fully implicit scheme was used for the time integral with time step of 0.005 s. The detailed numerical procedure and calculation domain have been given somewhere else [18]. Model assumptions have also been given previously [19].

4. Results and Discussion

4.1 Effect of pressure on weight loss

Figure 2 (a) – (e) shows the weight loss history of the biomass material at different reactor pressures [0.0001, 0.01, 10 and 100 atm, representing vacuum (0.0001 and 0.01 atm), atmospheric (1 atm) and pressurized (10 and 100 atm) regions]. When reactor pressure was 0.0001 atm (Fig. 2a), active disintegration of biomass sample began at about 10 s elapsed time and continued until about 49 s. After 50 s, weight loss seemed to be constant for the remaining time until the process was terminated at about 60.5 s. As in thermally thin regime [14], the weight loss history profile was similar at all other reactor pressures considered. This implies that a change in reactor pressure during biomass pyrolysis does not significantly affect the primary reactions of the feedstock even in thermally thick regime. However, unlike in thermally thin regime, pyrolysis time was elongated at 100 atm by 7.5 s (Figure 2 (e)). It is possible that at this reactor pressure, external heat transfer resistance is a little higher than at other reactor pressures. A further study may be required to fully understand this scenario.

4.2 Primary tar production rate

Figure 3 shows primary tar production rate at different reactor pressures. From the figure, primary tar production rate profiles are the same in all cases. As shown in the pyrolysis mechanism (Figure 1), primary tar production reaction is one of the three parallel and competing initial reactions undergone by the biomass sample. This result suggests further that, just as in thermally thin regime, changes in reactor pressure do not also have any significant effect on the primary pyrolysis of woody biomass in thermally thick regime.

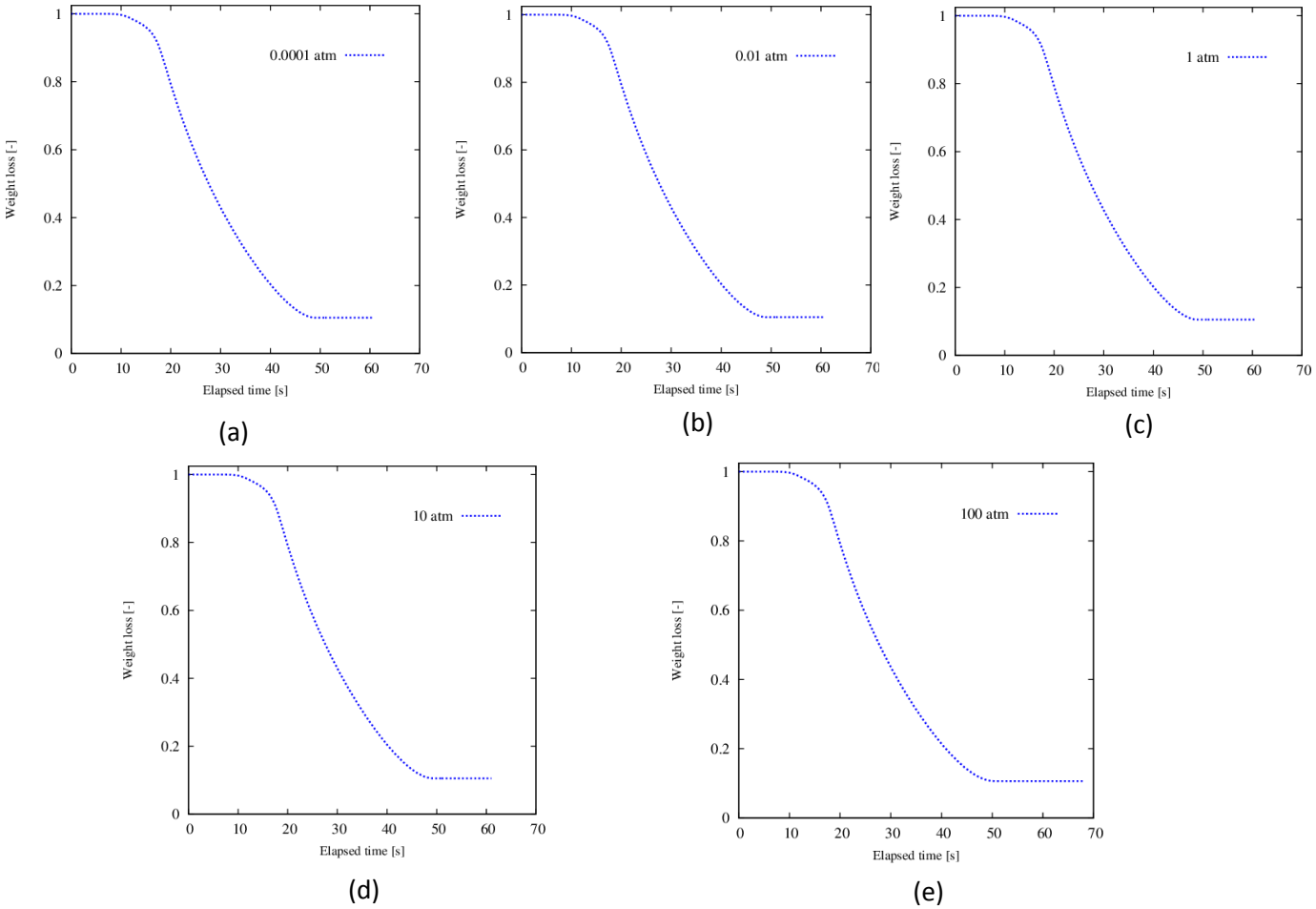

Figure 2: Weight loss history at different reactor pressures; (a) at 0.0001 atm, (b) at 0.01 atm, (c) at 1 atm (d) at 10 atm, (e) at 100 atm

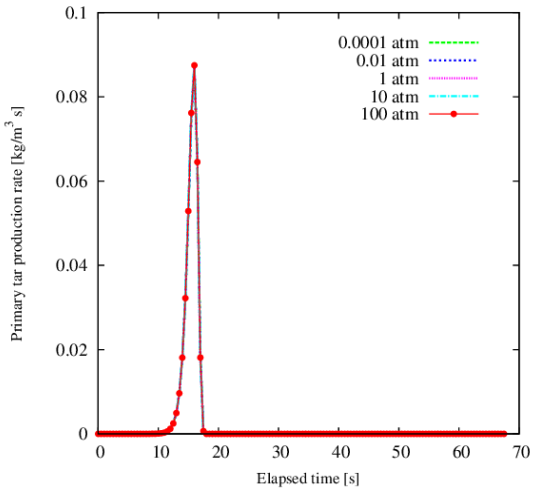

Figure 3: Primary tar production rate at different reactor pressures

4.3 Primary tar secondary reactions

Unlike in thermally thin regime, where there is no temperature gradient within the pyrolyzing solid, it is expected that in thermally thick regime, the presence of temperature gradient will affect intra-particle volatile transport and chemical kinetics of secondary reactions. Figure 4 shows the rate of products generation from

primary tar intra-particle secondary reactions at different reactor pressures. As shown in the figure, there was no increase in the rate of secondary products generation with pressure increase in the vacuum region (0.0001 – 0.01 atm). This is similar to our findings in the thermally thin regime [14]. However, there is only one peak instead of two in the thermally thin regime. Furthermore, the rate of secondary products generation in the pressurized region is not significantly different from that at atmospheric condition while at the same time, the peak at 10 atm appears to be a little higher than that at 100 atm. In order to clarify this scenario, the temperature profile at the centre of the biomass sample was simulated at different reactor pressures. As shown in Figure 5, the temperature profiles at the centre of the sample for all the conditions under study were uniform until about 40 s, after which pressure increase resulted in decrease in temperature gradient. This became more conspicuous with pressure increase from 10 atm to 100 atm.

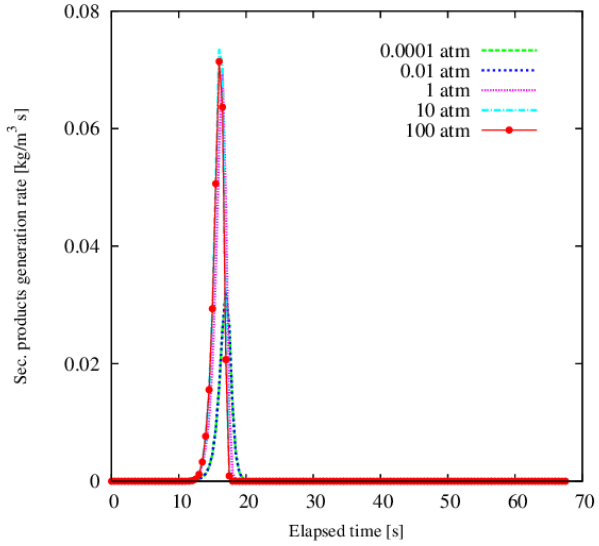

Figure 4: Rate of products generation from primary tar secondary reactions

From chemical kinetics standpoint, decrease in intra-particle temperature gradient has a lot of implications as far as intra-particle secondary reactions are concerned. This suggests that at vacuum and atmospheric regions, within some time interval, more tar molecules will be consumed as they flow towards the heated surface than at pressurized region.

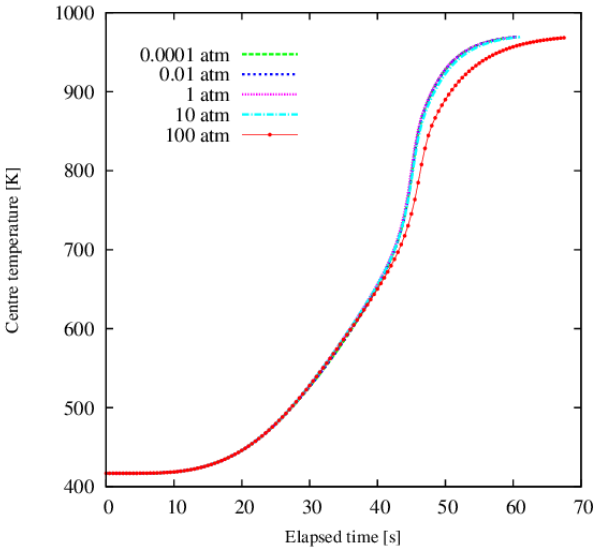

Figure 5: Temperature history at the centre of the biomass sample at different reactor pressures

4.4 Tar release rate

Figure 6 shows the rate of tar release at different reactor pressure. From the figure, as in thermally thin regime, the rate of tar release is highest in the vacuum region (where reactor pressure is less than 1 atm). At this region, increase in pressure did not have any effect on the rate of tar release (i.e. tar yield is not sensitive to pressure increase in this region). As the reactor pressure increased from vacuum to atmospheric, there was a significant reduction in the rate of tar release. This is as a result of more tar molecules participating in intra-particle secondary reactions to yield secondary tar, more gas and char. As the reactor pressure increased above atmospheric, there was a further decrease in the rate of tar release from the pyrolyzing solid. This is due to the fact that a higher percentage of tar produced from primary pyrolysis was consumed in intra-particle secondary reactions. Aside from increase in pressure, the particle size is also contributory because in large particles, time duration for tar transport within the pyrolyzing solid is elongated thereby making more time available for intra-particle secondary reactions. In the pressurized region (region above atmospheric condition), further increase in pressure does not have any significant effect on tar release rate. Furthermore, as shown in the figure, tar release rate, after getting to its maximum value reduces until it becomes negative in all the regions considered, the negative peak varying from one region to another, the maximum being at atmospheric and the minimum at 100 atm. This implies that as tar molecules flow towards the heated surface to escape from the pyrolyzing solid, they are being consumed in intra-particle secondary reactions. Grønli and Melaaen [20] have reported a similar observation. Negative peaks did not occur in thermally thin regime [14].

4.4 Gas release rate

Figure 7 shows the rate of gas release at different reactor pressures. From the figure, below atmospheric, i.e. vacuum region (0.0001 and 0.01 atm), increase in reactor pressure has no noticeable effect on gas release rate. This is similar to our findings in thermally thin regime [14]. When reactor pressure increased from vacuum to atmospheric however, there was a sharp increase in gas release rate from the pyrolyzing solid. As pyrolysis condition became pressurized, unlike in thermally thin regime, there was no noticeable difference in gas release rate.

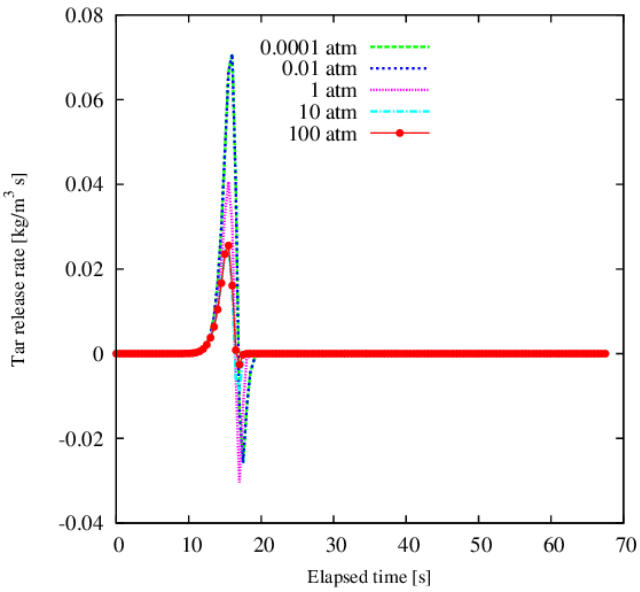

Figure 6: Tar release rate at different reactor pressures

This may be due to the fact that more tar molecules are consumed during intra-particle secondary reactions at atmospheric than at pressurized condition (P = 10 atm) within some time frame (Figure 6), yielding more gas. Further increase in reactor pressure from 10 atm to 100 atm caused a slight reduction in the peak of gas release rate. As earlier explained, reduction in temperature gradient with increasing pressure during pyrolysis can significantly affect the distribution and composition of the products. Although one would possibly suggest

increase in resistance to external heat transfer as reactor pressure increases, there is need for further study to clarify what brought about this reduction in temperature gradient.

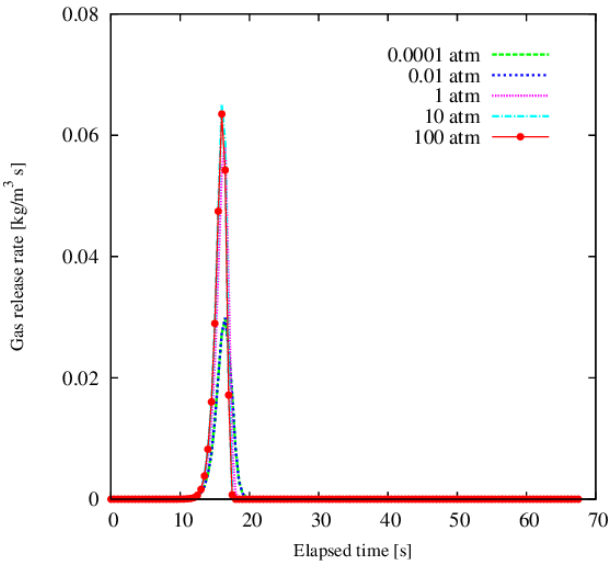

Figure 7: Gas release rate at different reactor pressures

5. Conclusions

Effects of reactor pressure in thermally thick regime have been investigated. For large biomass particles subjected to convective-radiative heating at 30 K/s and final reactor temperature 973 K, increase in reactor pressure does not affect the rate of primary tar generation. Findings also revealed that increase in pressure reduces intra-particle temperature gradient (more pronounced as pressure increased to 100 atm) resulting in momentary consumption of a higher percentage of tar molecules in vacuum and atmospheric regions than in pressurized region during intra-particle secondary reactions as tar molecules migrate towards the particle surface. Although there is some clear difference between the positive and negative peaks of tar release rates at atmospheric and pressurized regions, there is no significant difference in the rate of gas release for both regions. These results have shown that there may be no significant difference in products yield distribution in thermally thick regime between atmospheric and pressurized pyrolysis conditions.

Nomenclature

A: pre-exponential factor	(1/s)
B: permeability	(m^2)
Cp: specific heat capacity	(J/ kg K)
E: activation energy	(J/mol)
e: emissivity	(-)
h_c: convective heat transfer coefficient	(W/ m^2 K)
k: reaction rate constant	(1/s)
k_c: char thermal conductivity	(W/m K)
k_w: wood thermal conductivity	(W/m K)
M: molecular weight	(kg/mol)
P: Pressure	(Pa)
Q: heat generation	(W/m^3)
Q_c: convective heat flux	(W/m^2)
Q_r: radiation heat flux	(W/m^2)
R: universal gas constant	(J/mol K)
R: total radial length	(m)

r: radial direction
z: axial direction
S: source term
T: temperature (K)
t : time (s)
U: axial velocity component (m/s)
V: radial velocity component (m/s)
ε: porosity (-)
ε_0: initial porosity (-)
Δh: heat of reaction (kJ/kg)
μ: viscosity (kg/m s)
ρ: density (kg/m^3)
ρ_{w0}: initial density of wood (kg/m^3)
σ: Stefan-Boltzmann constant ($W/m^2 K^4$)
η: degree of pyrolysis

Subscripts
Ar: Argon
c: char, primary char formation reaction
c_2: secondary char formation reaction
g: gas, primary gas formation reaction
g_2: secondary gas formation reaction
is: intermediate solid, intermediate solid formation reaction
s: solid
t: tar, tar formation reaction
v: total volatile
w: wood

References

[1] Lu, H., Ip, E., Scott, J., Foster, P., Vickers, M. and Baxter, L.L. (2010). Effects of Particle Shape and Size on Devolatilization of Biomass particle. *Fuel* **89**, 1156-1168.

[2] Chan, W.R., Kelbon, M. and Krieger, B.B. (1985). Modelling and Experimental Verification of Physical and Chemical Processes during Pyrolysis of a Large Biomass Particle. *Fuel* **64**, 1505-1513.

[3] Liliedahl, T. and Sjöström, K. (1998). Heat Transfer Controlled Pyrolysis Kinetics of a Biomass Slab, Rod or Sphere. *Biomass and Bioenergy* **15(6)**, 503-509.

[4] Fushimi, C., Araki, K., Yamaguchi, Y. and Tsutsumi, A. (2003). Effect of Heating Rate on Steam Gasification of Biomass. 2. Thermogravimetric-Mass Spectrometic (TG-MS) Analysis of Gas Evolution. *Industrial Engineering Chemistry Research* **42**, 3929-3936.

[5] Papadikis, K., Gu, S. and Bridgwater, A.V. (2009). CFD Modelling of the Fast Pyrolysis of Biomass in Fluidized Bed Reactors. Modeling the Impact of Biomass Shrinkage. *Chemical Engineering Journal* **149**, 417-427.

[6] Bharadwaj, A., Baxter, L.L. and Robinson A.L. (2004). Effects of Intraparticle Heat and Mass Transfer on Biomass Devolatilization: Experimental Results and Model Predictions. *Energy & Fuel* **18**, 1021-1031.

[7] Hagge M.J. and Bryden, K.M. (2002). Modeling the Impact of Shrinkage on the Pyrolysis of Dry Biomass. *Chemical Engineering Science* **57**, 2811-2823.

[8] Park, W.C., Atreya, A. and Baum, H.R. (2010). Experimental and Theoretical Investigation of Heat and Mass Transfer during Wood Pyrolysis. *Combustion and Flame* **157**, 481-494.

[9] Babu, B.V. and Chaurasia, A.S. (2003). Modeling for Pyrolysis of Solid particle: Kinetics and Heat Transfer Effects. *Energy Conversion and Management* **44**, 2251-2275.

[10] Antal, M.J. (1983). Effects of Reactor Severity on the Gas-phase Pyrolysis of cellulose and Kraft Lignin-derived Volatile Matter. *Industrial Engineering Production Research and Development* **22**, 366-375.

[11] Scotts, D.S., Piskorz, J., Bergougnou, M.A., Graham, R. & Overend, R.P. (1988). The Role of Temperature in the Fast Pyrolysis of Cellulose and Wood. *Industrial Chemistry Research* **27**, 8-15.

[12] Pyle, D.L.and Zaror, C.A. (1984). Heat Transfer and Kinetics in the Low Temperature Pyrolysis of Solid. *Chemical Engineering Science* **19**, 147-158.

[13] Horne, P.A. and Williams, P.T. (1996). Influence of Temperature on the Products from the Flash Pyrolysis of Biomass. *Fuel* **75**, 1051-1059.

[14] Okekunle, P.O. and Osowade E.A. (2014). Numerical Investigation of the Effects of Reactor Pressure on Biomass Pyrolysis in Thermally Thin Regime. *In Press, International Journal of Chemical and Process Engineering Research.*

[15] Ståhl, M., Granström, K., Berghel, J. and Renström, R. (2004) Industrial Processes for Biomass Drying and their Effects on the Quality Properties of Wood Pellets. *Biomass and Bioenergy* **27(6)**, 621-628.

[16] Di Blasi, C. (2008) Modeling Chemical and Physical Processes of Wood and Biomass Pyrolysis. *Progress in Energy and Combustion Science* **34**, 47-90.

[17] Okekunle, P.O., Watanabe, H., Pattanotai, T. & Okazaki, K. (2012). Effect of Biomass Size and Aspect Ratio on Intra-particle Tar Decomposition during Wood Cylinder Pyrolysis. *Journal of Thermal Science and Technology* **7(1)**, 1-15.

[18] Okekunle, P.O., Pattanotai, T., Watanabe, H. and Okazaki, K. (2011). Numerical and Experimental Investigation of Intra-particle Heat Transfer and Tar Decomposition during Pyrolysis of Wood Biomass. *Journal of Thermal Science and Technology* **6(3)**, 360-375.

[19] Okekunle, P.O. (2013). Numerical Investigation of the Effects of Thermo-physical Properties on Tar Intra-particle Secondary Reactions during biomass Pyrolysis. *Mathematical Theory and Modeling* **3(14)**, 83-97.

[20] Grønli, M.G. and Melaaen, M.C. (2000) Mathematical Model for Wood Pyrolysis – Comparison of Experimental Measurements with Model Predictions. *Energy & Fuels* **14,** 791-800.